ARCHIVES

o f

FOUNDRY ENGINEERING

Analysis of Thermal Stability of Intermetallic Phases Precipitates in Continuous Ingots of AlCu4MgSi Alloy

P.M. Nuckowski [a], *, M. Kondracki [b], T. Wróbel [b]

[a] Institute of Engineering Materials and Biomaterials, Silesian University of Technology,
Konarskiego 18A, 44-100 Gliwice, Poland
[b] Department of Foundry Engineering, Silesian University of Technology,
Towarowa 7, 44-100 Gliwice, Poland
* Corresponding author. E-mail address: pawel.nuckowski@polsl.pl

Abstract

The article presents the results of research concerning to AlCu4MgSi alloy ingots produced using horizontal continuous casting process. The presented research was focused on the precise determination of phase composition of the precipitates formed during the solidification of ingots and the analysis of their thermal stability. In order to assess the morphology of precipitates in the AlCu4MgSi alloy, data obtained by using a computer simulation of thermodynamic phenomena were compiled with results obtained using advanced research techniques, i.e. High-temperature X-ray diffraction (HT-XRD), SEM-EDS, Thermal and derivative analysis (TDA) and Glow discharge optical emission spectroscopy (GD OES). SEM observations and analysis of chemical composition in micro-areas showed that the precipitates are mainly intermetallic θ-Al_2Cu and β-Mg_2Si phases, and also presence of $Al_{19}Fe_4MnSi_2$ intermetallic phase was confirmed by X-ray diffraction studies. Based on the prepared Thermo-Calc simulation data, high-temperature X-ray diffraction measurements were conducted.

Keywords: Aluminium alloys, phase analysis, High-temperature X-ray diffraction (HT-XRD), Thermal-derivative analysis (TDA)

1. Introduction

Aluminium-copper alloys (called duralumins) are characterized by high stength-to-weight ratio, which can be increased by heat treatment. They are widely used in many branches of industry, mainly automotive, aircraft and construction. For the production of finished or semi-finished product from Al-Cu alloys foundry technologies are used, such as gravity die casting [1] and semi-continuous and continuous casting [2]. With the use last mentioned technology, semi-product in the form of ingots are mainly produced, which are next subjected to plastic working and heat treatment, in order to obtain required mechanical properties. The technology of continuous casting has many advantages in this respect. In this process, the ingot is obtained by a controlled flow of molten metal through the crystallizer. The flowing metal, while dissipating heat through the walls of the crystallizer, changes its physical state from liquid to solid in a continuous way. An important advantage of this technology is the flexibility of parameter control and the possibility of integration with other processes, i.e. plastic working and heat treatment. Therefore, a very important factor in the production and further processing of continuous ingots of Al-Cu

alloys is the proper understanding, the predictive modeling and the control of phase morphology and evolution [3].

2. Description of research

The presented research was focused on the precise determination of phase composition of the precipitates formed during the solidification of AlCu4MgSi alloy continuous ingots and the analysis of their thermal stability. Depending on the casting conditions and elemental composition of Al-Cu alloy, iron may leads to the formation of various intermetallic phases, which affect to workability. Due to the low solubility of iron in aluminium, during the crystallization of the alloy the intermetallic phases are formed, which contain Al, Mn, Fe, Si, Cu, and are generally stable at high temperature [4, 5]. The iron-rich intermetallic phases that appear in the microstructure reduce the tensile strength and the ductility of the alloys [6].

The most common phases in Al-Cu alloys in the as-cast state are the Al_2Cu (θ) precipitates [3, 5] which are the main strengthening phases in precipitation hardening [7]. Presence of Mg and Si in Al-Cu alloys, may lead to formation of β-Mg_2Si and wide variety of Q(Al-Cu-Mg-Si) phases [8, 9]. The intermetallic phases formation in this alloys is also highly dependent on the Cu and Mg content, determined by Cu/Mg ratio [10].

In order to assess the morphology of precipitates in the AlCu4MgSi alloy, data obtained using the computer simulation of thermodynamic phenomena was compiled with results obtained with advanced research techniques, i.e. High-temperature X-ray diffraction (HT-XRD), SEM-EDS, Thermal and derivative analysis (TDA) and Glow discharge optical emission spectroscopy (GD OES). Collected data will be used in future research aimed to determine plastic and thermal treatment process conditions of described continuous ingots.

3. Material and methodology

Tests were carried out on AlCu4MgSi (EN AW-2017A) alloy ingots (30 mm in diameter), which were produced using an aluminium alloys horizontal continuous casting test stand, located in the technological laboratory of the Department of Foundry Engineering at Silesian University of Technology. Detailed description of implemented horizontal continuous casting process and parameters is presented in previous works of the authors [11, 12].

Chemical composition of the ingots (Tab. 1) was analysed by means of glow discharge optical emission spectroscopy (GD OES), using a LECO GDS 500 spectrometer. The observations of ingot structure and the chemical composition analysis in micro-areas, were performed with the use of a Phenom ProX scanning electron microscope equipped with EDS detector. The high-temperature qualitative phase analysis of samples was based on X-ray diffraction measurements, performed with the use of a Panalytical X'Pert Pro MPD diffractometer equipped with Anton Paar HTK 16 high-temperature chamber. Measurements were carried out in the temperature of 25°C and 530°C, heating and cooling conditions of the samples are shown in the graph (Fig. 1). In the XRD measurements filtered radiation of a copper-anode

lamp was used (λK_α= 0.154 nm), and a PIXcell 3D detector on the diffracted beam axis. Diffraction lines of AlCu4MgSi alloy, were recorded in the angular range of 15-55° [2θ], at step = 0.026° and count time per step = 400s. Analyses were performed using Panalytical High Score Plus software with dedicated PAN-ICSD database. Thermal and derivative analysis (TDA) was performed on prepared cylindrical samples (18 mm in diameter and 20 mm length) using Universal Metallurgical Simulator and Analyzer (UMSA) device. Samples were melted at 700°C under argon protective atmosphere. Followed by isothermal 90 s holding , all the melts were solidified and cooled to ambient temperature in the crucibles with argon protection in the furnace to minimize the oxidation. Signal from the thermal and derivative analysis was acquired using a high-speed National Instruments data acquisition system. K-type thermocouple was used in all the experiments. Test samples were solidified at a cooling rate of approximately 0.5°C/s, equivalent to the solidification process under natural cooling.
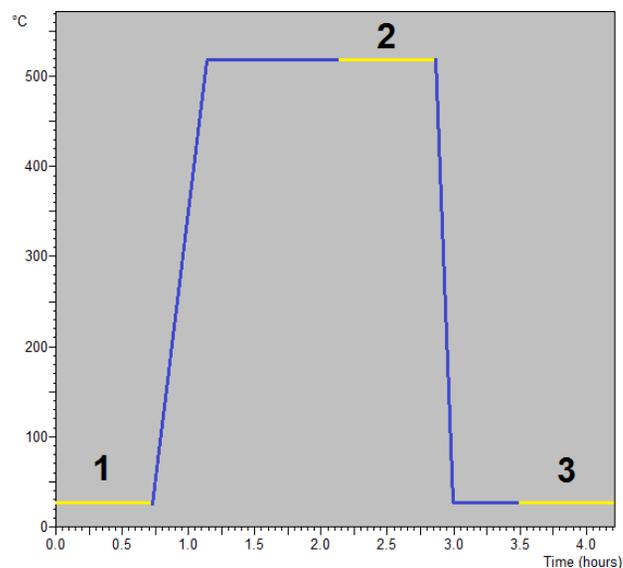

Fig. 1. Heating and cooling conditions of AlCu4MgSi alloy samples during the High-temperature X-ray diffraction measurements (HT XRD)

4. Results and discussion

Chemical composition of examined Al-Cu alloy was shown in Table 1. The obtained results confirmed that the tested ingots can be classified as ISO: AlCu4MgSi (AW-2017A, PN-EN 573-3 standard).

The numerical modelling consisted of several simulations in equilibrium state for the alloy with chemical composition obtained in the analysis. First calculations were aimed to determine the crystallization process and the sort and amount of phases occurring during this process. Next the chemical composition of the phases in function of temperature was calculated. Finally, the influence of slight changes of alloying

element content on the structure and characteristic temperatures was studied.

In Fig. 2 the phase fraction in function of temperature can be seen. The diagram enables the identification of liquidus (638°C) and solidus temperature (530°C) and the description of the crystallization path. The leading phase in this process is the α phase, occurring at 638°C and crystallizing up to the solidus temperature. Along , other phases occur. After the liquid volume reaches the level of aprox. 50%, the intermetallic phase $Al_{13}Fe_4$ crystalizes at 616°C. With liquid level of 25% at 603°C Al_6Mn phase occur. Last phase in the primary crystallization is the Mg_2Si (liquid level aprox. 5%, temperature: 544°C). During the secondary crystallization two phase transformations take place; the first one is connected with θ phase at 505°C. The second transformation is $Al_6Mn \rightarrow Al_{12}Mn$ at 350°C.

The chemical composition of the structural components is not strongly influenced by the temperature. The biggest changes are observed in the α phase and the Cu content, what is connected with the θ phase crystallization in the solid state.

Small changes in the content of the alloying elements do not influence significantly the characteristic temperatures and the occurring phases.

One of the method used to compare the calculated route of crystallization with the experimental results was the Thermal and Derivative Analysis. In Fig. 3 the TDA curves can be seen. During the analysis the temperature is registered on function of time (cooling curve) and next its first derivative after time is calculated (crystallization curve). The characteristic points in the crystallization curve enable to describe the crystallization process of the alloy. Each change in the curve is connected with the heat effect of some phase transformation. In most cases such heat

effect can be described by 3 or 4 points [13]. The main heat effect is in the analysed alloy connected with α phase crystallization (points A-B-H). During the primary crystallization two other heat effects can be observed. Points C-D-E show a small thermal effect in the first stage of the crystallization. Points F-G-H show a distinct heat effect of crystallization just before the solidus temperature. During the secondary crystallization only one effect is observed, connected with θ phase crystallization and described by points I-J-K.

Scanning electron microscope (SEM) observations (Fig. 4) allowed the assessment of the morphology of precipitates. The observed precipitates in form of a complex shape lattice, were mainly located in the interdendritic regions. To determine the morphology and the type of non-equilibrium phase forming a precipitates lattice in the structure of analysed alloy, energy dispersive X-ray spectroscopy (EDS) was applied. The analysis (Fig. 5, Table 2) shown significant differences of chemical composition in the precipitate micro-areas (Fig. 4) which can be also observed as a variation in contrast. Presence of bright copper-rich regions (precipitates marked with points 7 and 8) indicates to θ-Al_2Cu phase. The magnesium and silicon-rich dark, punctual precipitates observed in this same region, are probably the β-Mg_2Si phase. The grey Mn and Fe-rich areas marked with points 6, 8 and 10, are presumably complex multi-component phases. According to [6] the reaction of manganese with iron in the cast alloy, formed the iron-rich intermetallic multi-component phases. These iron-rich intermetallic compounds appeared in microstructure after casting process in various forms and type depending on manganese amount.

Table 1.
Chemical composition of AlCu4MgSi (EN AW-2017A) alloy

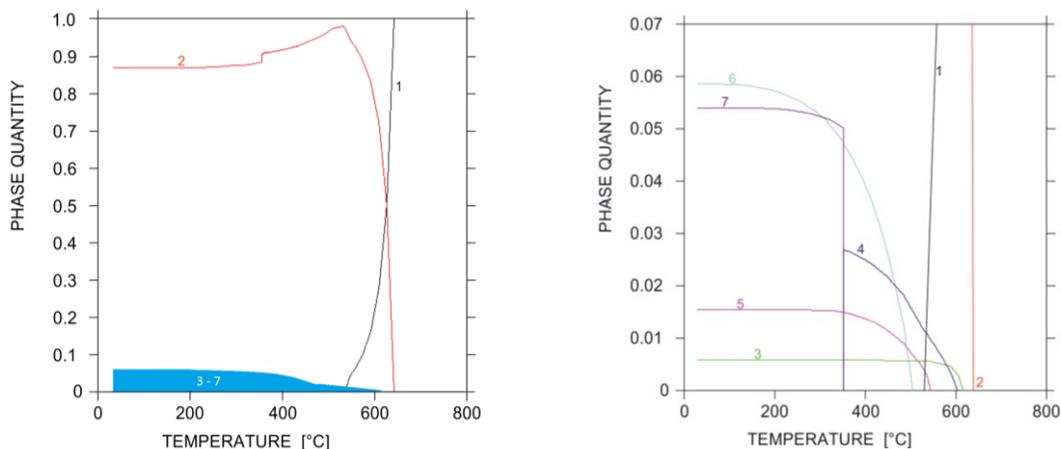| Material designation			elements concentration [% wt.]									
ISO:	EN:	Element	Si	Fe	Cu	Mn	Mg	Cr	Zn	other	Zr+Ti	Al
AlCu4MgSi	AW-2017A	min.	0,2	≤ 0,7	3,5	0,4	0,4	≤ 0,1	≤ 0,25	≤ 0,15	≤ 0,25	balance
		max.	0,8		4,5	1,0	1,0					
Tested ingots (GD OES)			0,52	0,28	4,45	0,82	1,00	0,05	0,22	0,03	0,01	balance

Fig. 2. Results of numerical simulation for the studied alloys. Volume fraction of occurring phases in function of temperature. Full diagram (left), magnification (right). 1 – liquid, 2 – α phase, 3 – $Al_{13}Fe_4$, 4 – Al_6Mn, 5 – Mg_2Si, 6 – Al_2Cu (θ phase), 7 – $Al_{12}Mn$
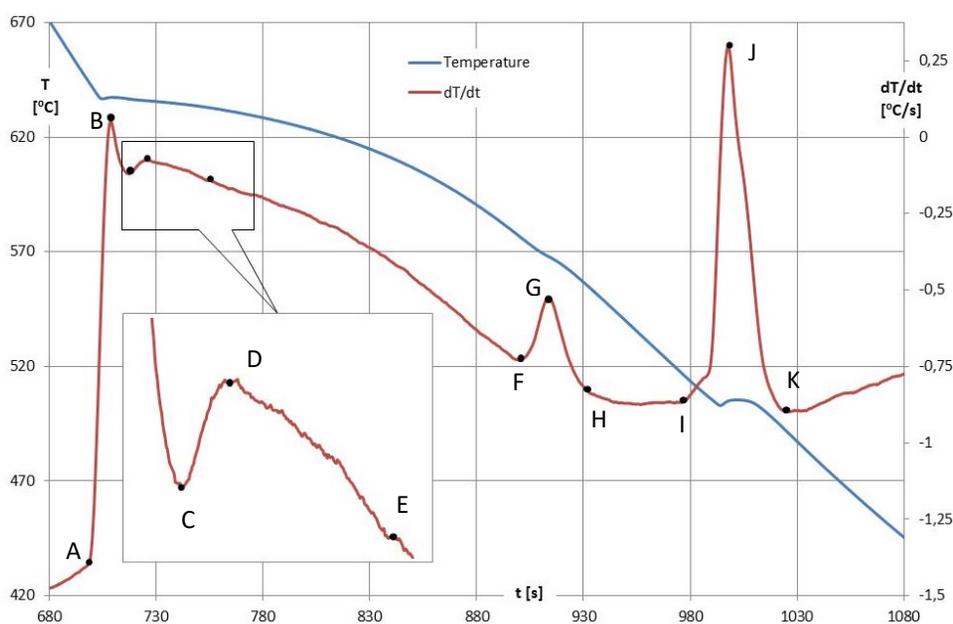
Fig. 3. Thermal and derivative analysis curves for the studied alloy. The cooling curve $T = f(t)$ and the crystallization curve $dT/dt = f(t)$ with indicated characteristic points. Full description in the text
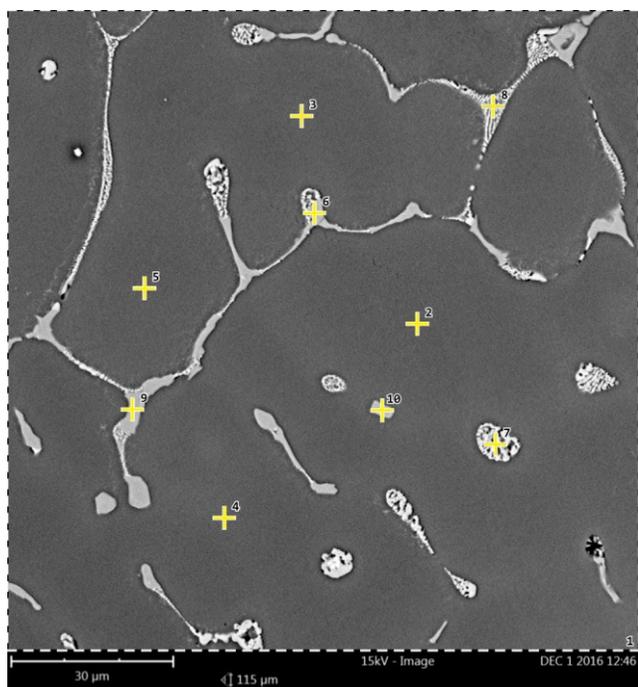

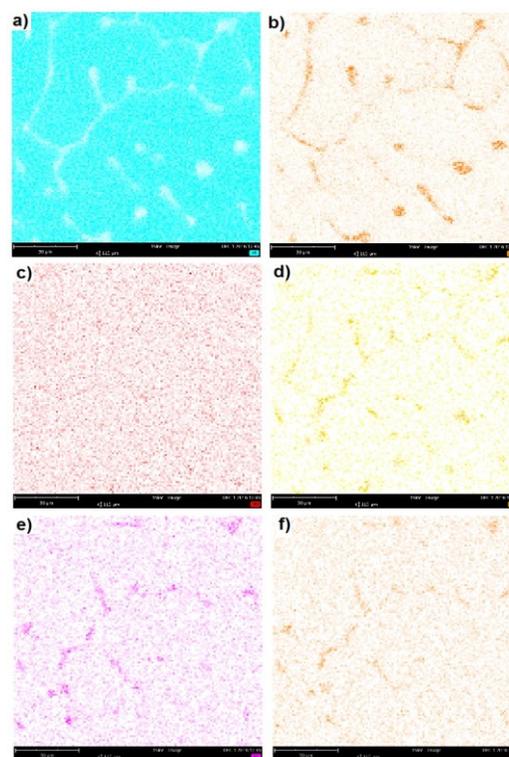Fig. 4. Structure of the AlCu4MgSi alloy ingots

Fig. 5. Results of chemical composition analysis for area shown in Fig. 4. Map for: a) Al, b) Cu, c) Mg, d) Si, e) Fe, f) Mn

Table 2.
Results of chemical composition analysis for area shown in Fig. 4

Point of analysis (Fig. 2)	Elements concentration [% at.]					
	Al	Cu	Mg	Si	Fe	Mn
1	95,9	1,6	1,4	0,4	0,2	0,4
2	≈ 99	-	-	-	-	-
3	99,3	0,7	-	-	-	-
4	98,9	1,1	-	-	-	-
5	≈ 99	-	-	-	-	-
6	74,2	3,8	-	8,5	7,4	6,1
7	75,0	22,7	2,2	-	-	-
8	77,1	14,7	5,4	2,8	-	-
9	74,7	3,8	-	8,0	7,6	5,9
10	76,6	3,7	-	7,5	6,6	5,6

To confirm the presence of the assumed phases, X-ray diffraction qualitative analysis was conducted. Measurement performed at ambient temperature (Fig. 6) confirmed the presence of an α-Al solid solution, as well as the θ-Al$_2$Cu and β-Mg$_2$Si intermetallic phases. Also the quaternary Al$_{19}$Fe$_4$MnSi$_2$ intermetallic phase was determined. In order to determine thermal stability of the intermetallic phase precipitations, high-temperature X-ray diffraction measurements were performed. The temperature (530°C) was selected to the basis on prepared Thermo-Calc simulations, as above the θ-Al$_2$Cu solubility temperature and below solidus. Before the measurement, the sample was held for one hour at the set 530°C and during the test temperature was maintained. The analysed diffractogram, registered for sample at 530°C (Fig. 7, red lines), did not shown diffraction lines connected to θ-Al$_2$Cu and β-Mg$_2$Si. Which indicates that these phases do not occur at this temperature. Diffraction lines observed at the Al$_{19}$Fe$_4$MnSi$_2$, shown that this intermetallic phase is stable at 530°C. Measurement performed at 25°C (Fig. 7, blue lines) after sample cooling at a rate of 60°C/min, confirmed the presence of θ-Al$_2$Cu and β-Mg$_2$Si. Intensity of diffraction lines for this θ and β phases, has decreased referring to sample measured at 25°C before heating (Fig. 7, green lines), which may indicate the partial dissolution.
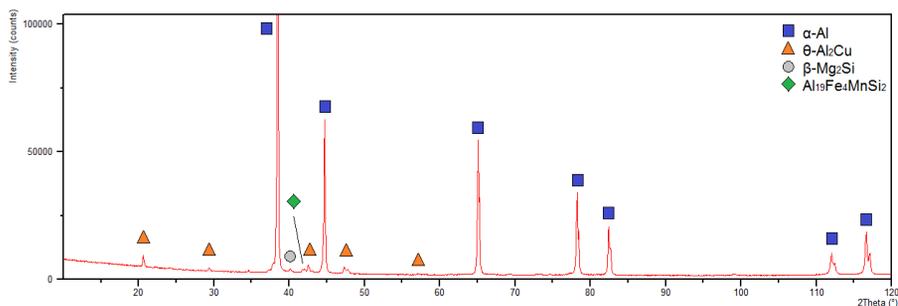

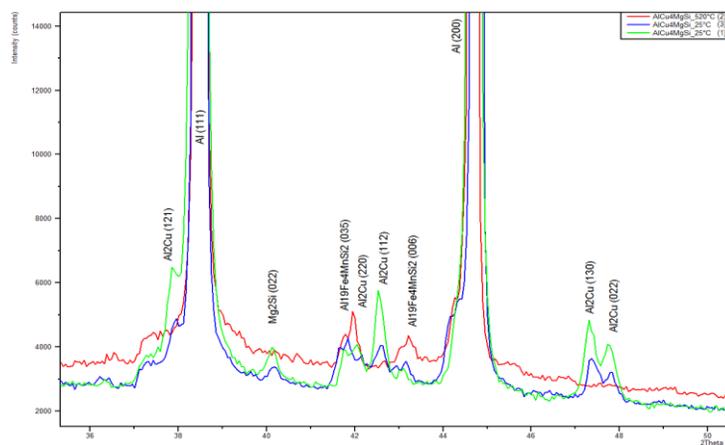Fig. 6. X-ray diffraction analysis of AlCu4MgSi alloy ingots

Fig. 7. High-temperature X-ray diffraction analysis of AlCu4MgSi alloy ingots, measurement conducted at temperature: 25°C (green line), 530°C (red line) and 25°C after heating and cooling (blue line)

Knowing what kind of phases are observed in the structure of the alloy, the crystallization process can be more precisely described. Taking into account the numerical simulation and the TDA results following crystallization path can be proposed; The leading phase in the process is the α phase crystalizing from the liquid and followed by the occurrence of the $Al_{19}Fe_4MnSi_2$ (effect C-D-E in Fig. 3). Although there is a discrepancy of the numerical results and experimental observations (lack of the Al_6Mn phase in the structure), analysing the composition of the quaternary phase one can see that the amount of the main elements equals the sum of calculated phases with additional amount of silicon ($Al_{13}Fe_4$ + Al_6Mn + Si_2), which is very active in the systems with iron or manganese [14]. Before the solidus temperature there is another distinct heat effect, connected with Mg_2Si crystallization (points F-G-H). After the solidus temperature only one effect is observed – the θ phase precipitation.

5. Conclusions

Based on the conducted studies the following conclusions have been formulated:
1. Presence of an α-Al solid solution, as well as the θ-Al_2Cu and β-Mg_2Si intermetallic phases in the analysed AlCu4MgSi alloy ingots were confirmed. Also quaternary $Al_{19}Fe_4MnSi_2$ intermetallic phase was determined.
2. Fe and Mn additions in analysed alloy leads to formation $Al_{19}Fe_4MnSi_2$ intermetallic phase. High-temperature X-ray diffraction measurements shown that this intermetallic phase is stable at $530^{\circ}C$.
3. The crystallization process of the alloy was well described thanks to connected analysis of numerical and experimental results and very detailed structural analysis.
4. The leading phase of crystallization is the α phase. Two of the intermetallic phases occur during the primary crystallization: the quaternary phase $Al_{19}Fe_4MnSi_2$ and the β-phase Mg_2Si. The third phase – Al_2Cu crystalizes during the secondary crystallization, in the solid state.

References

[1] Talamantes-Silva, M.A., Rodríguez, A., Talamantes-Silva, J., Valtierra, S. & Colás, R. (2008). Characterization of an Al-Cu cast alloy. *Materials Characterization*. 59, 1434-1439.
[2] Katgerman, L. (2016). Developments in Continuous Casting of Aluminium Alloys. *Cast Metals*. 4(3), 133-139.
[3] Vaithyanathan, V., Wolverton, C. & Chen, L.Q. (2004). Multiscale modeling of θ' precipitation in Al–Cu binary alloys. *Acta Materialia*. 52(10), 2973-2987.
[4] Totten, G.E., MacKenzie, D.S. (ed.) (2003). *Handbook of Aluminum volume 1 Physical Metallurgy and Processes*. New York: Marcel Dekker Inc.
[5] Lachowicz, M.M., Leśniewski, T., Lachowicz, M.B., Jasionowski R. (2012). Processes of tribological, cavitational and corrossional wear of tested aluminium alloys applied in plastic working. *Tribologia*. 5, 85-95.
[6] Gencalp Irizalp, S., Saklakoglu, N. (2014). Effect of Fe-rich intermetallics on the microstructure and mechanical properties of thixoformed A380 aluminum alloy. *Engineering Science and Technology, an International Journal*. 17(2) 58-62.
[7] Prados, E.F, Sordi, V.L., Ferrante, M. (2013). The effect of Al2Cu precipitates on the microstructural evolution, tensile strength, ductility and work-hardening behaviour of a Al–4 wt.% Cu alloy processed by equal-channel angular pressing, *Acta Materialia*. 61(1), 115-125
[8] Wolverton, C. (2001). Crystal structure and stability of complex precipitate phases in Al–Cu–Mg–(Si) and Al–Zn–Mg alloys. *Acta Materialia*. 49(16), 3129-3142.
[9] Chang, K., Liu, S., Zhao, D., Du, Y., Zhou, L. & Chen, L. (2011). Thermodynamic description of the Al–Cu–Mg–Mn–Si quinary system and its application to solidification simulation. *Thermochimica Acta*. 512(1-2), 258-267.
[10] Zheng, Y., Xiao, W., Ge, S., Zhao, W., Hanada, S. & Ma, C. (2015). Effects of Cu content and Cu/Mg ratio on the microstructure and mechanical properties of Al-Si-Cu-Mg alloys. *Journal of Alloys and Compounds*. 649, 291-296.
[11] Nuckowski, P.M. & Wróbel, T. (2018). The influence of variable parameters of horizontal continuous casting on the structure of AlCu4MgSi alloy ingots. *Archives of Foundry Engineering*. 18(1), 196-202. (DOI: 10.24425/118837).
[12] Nuckowski, P.M. & Wróbel, T. (2019). Mechanical properties and fracture analysis of AlCu4MgSi alloy ingots obtained by horizontal continuous casting. *Archives of Metallurgy and Materials*. 64(1), 113-118. (DOI: 10.24425/amm.2019.126225).
[13] Król, M. (2019). Magnesium-Lithium Alloys with TiB and Sr Additions. *Journal of Thermal Analysis and Calorimetry*. (DOI: 10.1007/s10973-019-08341-2).
[14] Kondracki, M., Gawroński, J. & Szajnar, J. (2005). Role of the Intermetallic Phases in Technological Process of Fixture Brasses. *Journal of Materials Processing Technology*, 162/163. 332-335. DOI: https://doi.org/10.1016/j.jmatprotec.2005.02.076.